J Mater Sci (2010) 45:139–145
DOI 10.1007/s10853-009-3905-x

High-temperature pyrolysis of ceramic fibers derived from polycarbosilane–polymethylhydrosiloxane polymer blends with porous structures

Ken'ichiro Kita · Masaki Narisawa · Atsushi Nakahira · Hiroshi Mabuchi · Masayoshi Itoh · Masaki Sugimoto · Masahito Yoshikawa

Received: 26 May 2009 / Accepted: 15 September 2009

Abstract The polymer blends of PCS (polycarbosilane) and PMHS-h (polymethylohydrosiloxane with high molecular weight) were prepared by freeze-drying process of mixed benzene solution. Melt viscosity, mass loss, and gas evolution from prepared polymer blends were analyzed. A polymer blend of HSah15 (15 mass% PMHS-h to PCS) was melt-spun to fiber form, curing by thermal oxidation and pyrolyzed at various temperatures up to 1773 K. The obtained fibers were investigated by tensile tests, FE-SEM (field emission scanning electron microscope) observation, and XRD (X-ray diffraction) analysis. After pyrolysis at 1273 K, there were no pores in the cross section of the fiber derived from pure PCS; however, there were amounts of pores in the cross sections of the fiber derived from HSah15. After pyrolysis at 1773 K, the coarse β-SiC (silicon carbide) crystals were formed on the outside surface of the fiber derived from pure PCS; however, no remarkable β-SiC crystal were formed on the outside surface of the fiber derived from HSah15.

K. Kita (✉) · M. Narisawa · A. Nakahira · H. Mabuchi
Graduate School of Engineering, Osaka Prefecture University,
Sakai, Osaka 599-8531, Japan
e-mail: hz302@mtr.osakafu-u.ac.jp

M. Itoh
Fukushima National College of Technology, Iwaki,
Fukushima 970-8034, Japan

M. Sugimoto · M. Yoshikawa
Quantum Beam Science Directorate, Japan Atomic Energy
Agency, Takasaki, Gunma 370-1292, Japan

Introduction

In recent years, it was found that the fibers derived from polycarbosilane (PCS)–polymethylhydrosiloxane (PMHS) polymer blends often yield porous structure [1]. Such porous structure is mainly determined by desaturation process of decomposed gas from polymer melts during fiber spinning and pressure drop [2]. When melt-spinning was carried out at high-viscosity region, the fibers with the amount of nano-sized pores in its cross section were obtained [3].

Inclusion of such nano-sized pores in the fiber, however, may diminish tensile strength as defects. Anyway, the obtained porous fibers are expected not to be equal to the previous fibers derived from simple polycarbosilane. High-temperature decomposition process of such fibers derived from the polymer blends were probably influenced by incorporated siloxane parts in cross-linked and condensed polymer networks.

In this study, we shed light on high-temperature pyrolysis process of the fibers derived from PCS–PMHS-h (PMHS-h: high molecular weight PMHS) polymer blends to examine application of the synthesized fibers with nano-sized pores at high-temperature region beyond 1273 K. If such nanoporous fibers with available strength can be produced in a mass scale, the fiber will be useful as a heat-resistant catalyst support in the form of fabrics or felts [4].

Experimental procedure

Commercialized PMHS-h (KF-9901, Shin-etsu Chemicals Co., Ltd., Japan) was blended with PCS (NIPUSI-Type A, Nippon Carbon, Japan). The blend ratios of PMHS-h to PCS were 5–20 mass% for comparison. Polymer blend solutions in benzene were freeze-dried and white powders were obtained. These prepared polymer blends were identified as HSahxx (xx is the mass of contained PMHS-h).

Viscosities of polymer blends were measured by viscometer (RB-80R, Toki Sangyo Co., Ltd., Japan) in N_2 atmosphere. Thermogravimetric analysis of HSah15 at 533–573 K was performed by electronic balance (BP310P, Sartorius K.K., Germany) with electric furnace (ARF-50M, Asahi-Rika Corporation, Japan)in an Ar flow. The gases evolved from PCS and HSah15 heated at 573 K were measured by gas chromatographs (GC-8A, Shimadzu Corporation, Japan). While these experiments of viscosity, thermogravimetric analysis, and gas chromatographs, the heating rate of samples was fixed at 5 K/min up to 513 K and the speed above 513 K was 1 K/min and kept for 1 h per 10 K increase up to 573 or 538 K.

The polymer blend containing 15 mass% of PMHS-h was melt-spun into organic pre-ceramic fibers at 578 K with positive pressure of 0.10 atm. The positive pressure was adjusted by an Ar gas flow and a buffer tank. Fluctuations of temperature on the nozzle of the spinneret during melt spinning were ±5 K. Length and diameter of glass cell used for melt spinning was 260 mm × 26 mm. Diameter of spinning nozzle was about 0.8 mm. The temperature of top of the melt is 40 K higher than that of the bottom part [1]. The rotational speed of the drum for melt-spinning was beyond 8 m/s. The pre-ceramic fibers were cured by thermal oxidation. While the fibers were cured, the heating rate was 8 K/h up to 485 K under flowing air. IR spectra of HSah15 polymer, HSah15 fibers before curing and after thermal curing were obtained by FT-IR spectrometer (Spectrum GX, PerkinElmer Japan Co. Ltd.). Besides, as a standard fiber, PCS was melt-spin into fiber and the fiber was cured by the same condition as HSah15 fiber curing.

After the curing, the above fibers were pyrolyzed at 1273 K for 1 h in inert atmosphere and the pyrolyzed fibers were re-pyrolyzed at 1623, 1673, 1723, or 1773 K for 30 min under Ar flow. In this pyrolysis and heating, the heating rate was set at 200 K/h. The re-pyrolyzed fibers were observed by FE-SEM (S-4800 and S-3000, Hitachi Ltd., Japan). X-ray diffraction patterns of these fibers were obtained by a diffractometer (GeigerFlex Rad and CN2182D5, Rigaku Corporation, Japan). The tensile strength of these fibers were measured at room temperature using a tensile testing machine (Model-1305D, Aikoh Engineering) with a gauge length of 10 mm and a crosshead speed of 2 mm/min. The average tensile strength was obtained from the measured results of more than 20 filaments. The surface areas of these fibers were measured by B.E.T. method with an automatic surface area analyzer (Macsorb HM model-1201, Mountech Co., Ltd., Japan).

Result and discussion

Figure 1 shows the relationship between melt viscosity and temperature in PCS and HSah05–20. The viscosity of PCS decreased rapidly until 583 K and decreased moderately beyond 583 K. The viscosity of HSah05 polymer decreased rapidly until 573 K and slowly beyond 573 K. In the temperature range within 533–603 K, the viscosity of HSah05 was less than that of PCS. HSah10 reached 20 Pa s at 563 K, which enabled manufacturing of the polymer blend into fibers by melt-spinning. The viscosity of HSah15 was almost the same as that of HSah10. As for HSah20, the viscosity was always lower than that of HSah15 at the same temperature. The phase separation, however, slightly occurred in the melt of HSah20. It is suggested that PMHS plays a role of plasticizer and 15 mass% of PMHS is the limit of solubility in PCS. Thus, HSah15 was selected as the sample for the following experiment.

Table 1 shows the chemical composition of gases from PCS and HSah15 polymer accumulated in the cell after 573 K heating. The main component of the evolved gas from PCS and HSah15 was hydrogen gas and the amount of evolved gas from HSah15 was twice as much as that from PCS. However, some gaseous silicone compounds may be missed in this analysis method because of re-condensation of the compounds at some cool points.

Figure 2 shows the mass residues and ceramics yields of PCS, HSah15, and fibers after thermal oxidation curing, pyrolysis at 1273 K. The masses of PCS, HSah15, and fibers after melt-spinning were adopted as each standard, and the other mass residues and ceramics yields were expressed as the comparison to the each standard. The mass gains of each fiber after curing were about 4.4%. These

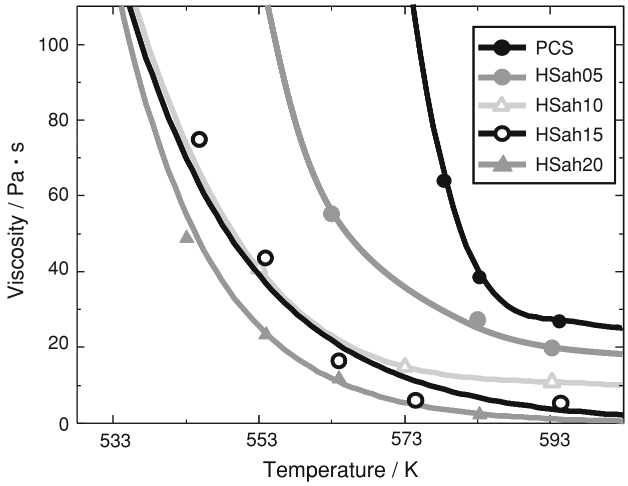

Fig. 1 The relationship between melt viscosity and temperature in PCS and HSah05–20

Table 1 Chemical composition of evolved gases from PCS and HSah15 after heating at 573 K

	PCS (mol/g)	HSah15 (mol/g)
Total	7.72×10^{-5}	1.35×10^{-4}
H_2	5.93×10^{-5}	1.30×10^{-4}
O_2	1.84×10^{-8}	4.55×10^{-9}
N_2	9.95×10^{-6}	2.24×10^{-7}
CH_4	1.12×10^{-6}	1.15×10^{-6}
CO	5.67×10^{-6}	3.31×10^{-6}
CO_2	1.20×10^{-6}	6.97×10^{-6}

(N_2: Background)

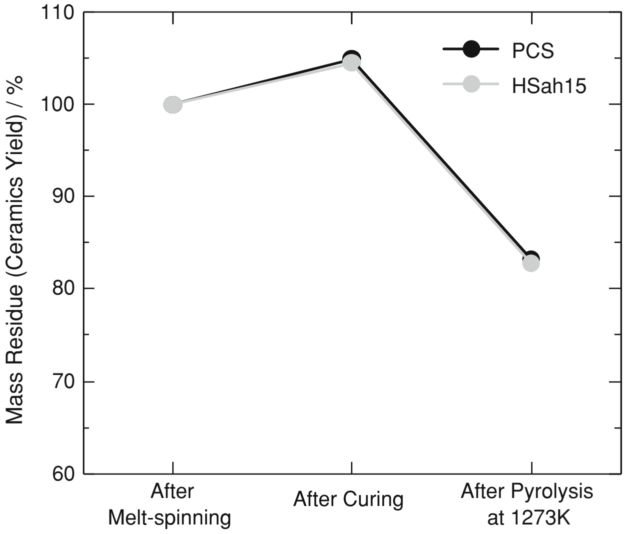

Fig. 2 The mass residues and ceramics yields of PCS and HSah15 after melt-spinning, curing, and pyrolysis at 1273 K

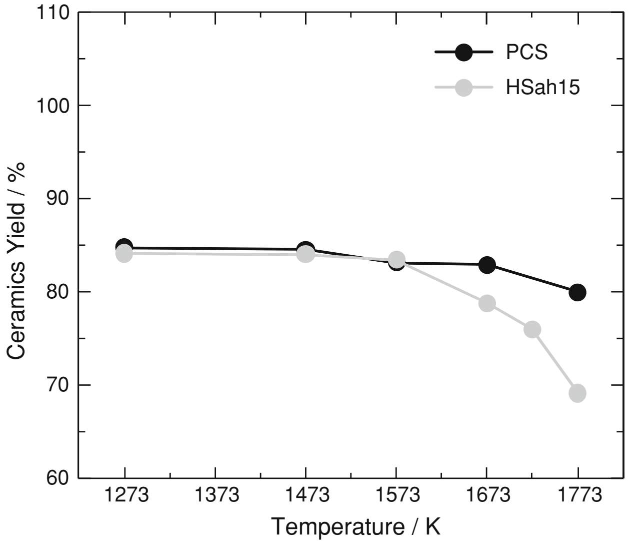

Fig. 3 The ceramics yields of PCS and HSah15 pyrolyzed at 1273–1773 K

mass gains were responsible for the oxidation which makes the cross-linking in polymers [5]. The ceramic yield of PCS fiber after pyrolysis at 1273 K was 83.1% and that of HSah15 fiber after pyrolysis at 1273 K was 82.8%. During the pyrolysis up to 1273 K, the main causes of the mass loss were known to be vaporization of low molecular weight silane oligomers up to 673 K, and methane evolution by methyl group decomposition at 873 K [6, 7]. Figure 3 shows the ceramics yields of PCS and HSah15 fibers after pyrolysis at 1273 K and re-pyrolyzed until 1773 K. These ceramics yields were compared to the each standard and the other ceramics yields were also compared to the each standard (Fig. 2). Both the ceramics yields re-pyrolyzed until 1573 K was almost the same; however, the ceramics yield of HSah15 re-pyrolyzed beyond 1573 K was less than that of PCS and the difference in residual masses tended to increase as the pyrolysis temperature increases. It is known that the mass loss in the Si–C–O fiber at such high temperature is accompanied by CO and SiO gas evolution [8]. During the CO–SiO gases evolution, microstructure change in the fiber, such as SiC crystallite growth, stacking of basic structure unit of carbon, and coarse grain precipitation on the fiber surface are known to proceed [9–11]. In this curing condition, the amount of oxygen captured in PCS and HSah15 was almost the same. The Si–C–O fiber derived from the polymer blends, however, contains much Si–O–Si bonds, because main chain of PMHS-h consists of Si–O–Si bonds. Such Si–O–Si bonds from PMHS-h are expected to be dispersed homogeneously in the spun, cure, and pyrolyzed fibers. Anyway, the amount of oxygen in cured HSah15 is larger than that in cured PCS. Therefore the difference of the whole ceramics yields of the fibers in the temperature range of

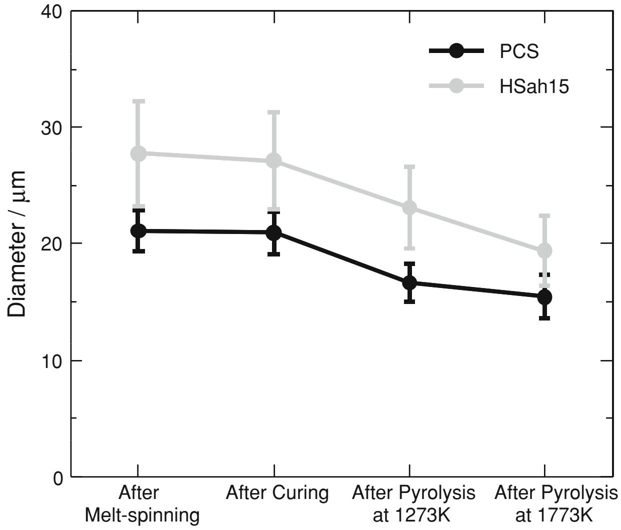

Fig. 4 The diameter of PCS, HSah15, and HSah15-1.2 atm after melt-spinning, curing, pyrolyzed at 1273 K and 1773 K

1573–1773 K is intrinsically caused by differences in CO and SiO gas evolution [12].

Figure 4 shows the diameters of PCS and HSah15 fibers after melt-spinning, curing, pyrolysis at 1273 K, and re-pyrolysis at 1773 K. The diameters of PCS and HSah15 fibers after melt-spinning were 21.1 and 27.8 μm. The diameter of PCS and HSah15 fiber after pyrolysis at 1273 K were 16.7 and 23.1 μm and that of PCS and HSah15 after re-pyrolysis at 1773 K were 15.4 and 19.4 μm. The diameter of HSah15 fiber after pyrolysis at 1273 K was 17% and that of HSah15 after re-pyrolysis at 1773 K was decreased by 32%. Considering Fig. 3, the tendency of diameter shrinkage during pyrolysis is roughly consistent with mass reduction of the fibers during pyrolysis.

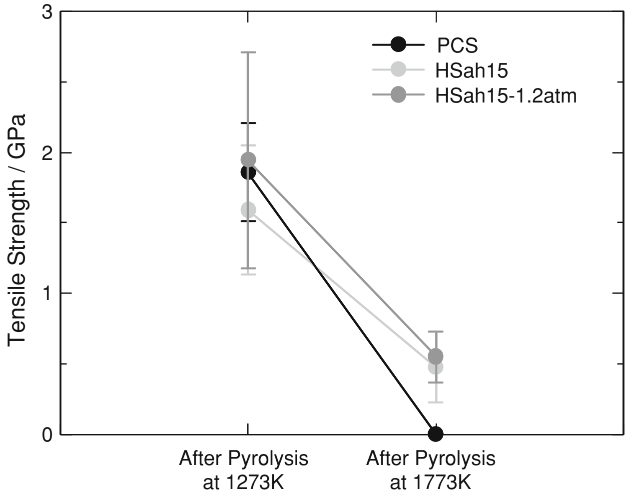

Fig. 5 The tensile strength of PCS, HSah15, and HSah15-1.2 atm fibers pyrolized at 1273 K and 1773 K

Figure 5 shows the tensile strength of PCS, HSah15 fiber pyrolyzed at 1273 K and re-pyrolyzed 1773 K. Tensile strength of HSah15-1.2 atm fibers (melt-spun with high pressure at 1.2 atm, 0.2 atm in the pressure was positive pressure) is also shown in the same figure as a reference. The tensile strength of PCS fiber pyrolyzed at 1273 K was 1.86 ± 0.35 GPa, but that of the fiber re-pyrolyzed at 1773 K was nearly 0 GPa. In the case of HSah15, the tensile strength of the fiber pyrolyzed at 1273 K was 1.59 ± 0.46 GPa and that of the fiber pyrolyzed at 1773 K was 0.47 ± 0.25 GPa. In spite of nano-sized pores in the fiber cross section, tensile strength of the nano-sized pore fiber was about 80% of that of the fiber derived from PCS. In addition, such nano-sized pore fiber held small tensile strength even after 1773 K heat treatment. It is beyond expectation, because the nano-sized pore fiber shows higher mass loss after high-temperature heat treatment. As for HSah15-1.2 atm, that of the fiber pyrolyzed at 1273 K was 1.95 ± 0.77 GPa and that of the fiber pyrolyzed at 1773 K was 0.55 ± 0.18 GPa. The increased strength of this fiber is explained by diminished pore number in the fiber cross section. Melt spinning with high pressure usually cause thinner fibers with decreased pore numbers.

Figure 6 shows the FE-SEM images of PCS, HSah15 fibers pyrolyzed at 1273 K in 1 h under inert atmosphere. There was no pore in the cross section of PCS, and there were the amounts of pores in the cross sections of HSah15.

Fig. 6 The FE-SEM images of PCS and HSah15 fibers pyrolized at 1273 K in 1 h under inert atmosphere

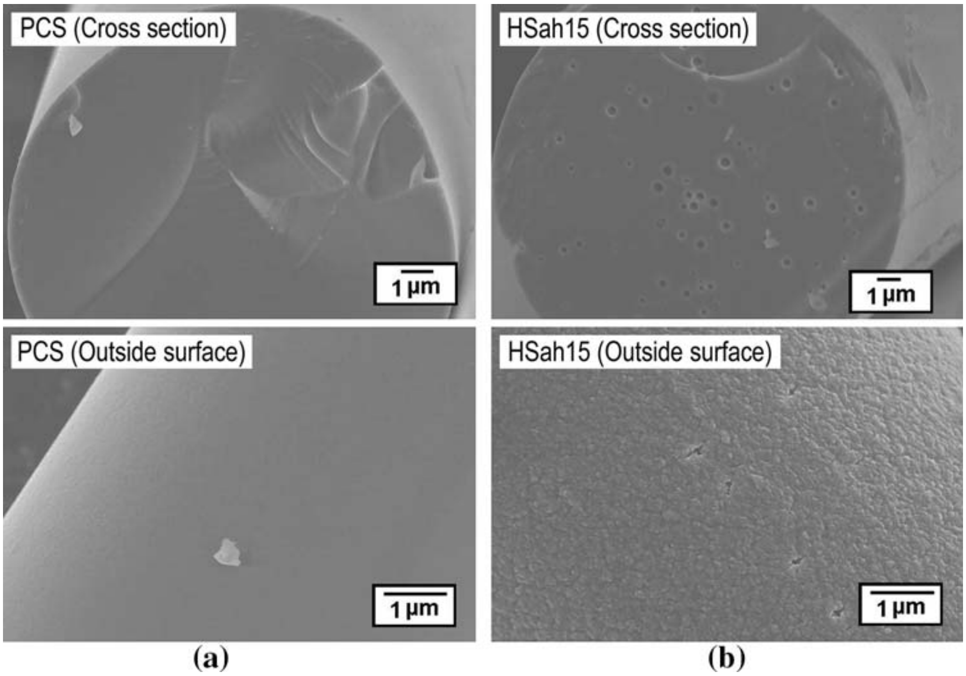

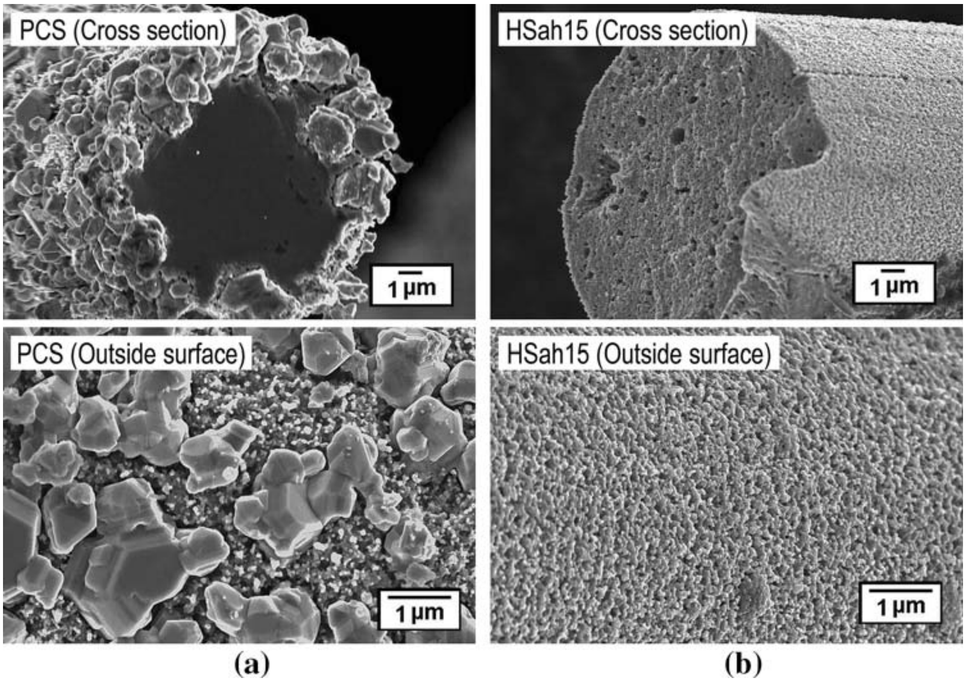

Fig. 7 The FE-SEM images of PCS and HSah15 fibers pyrolized at 1773 K in 0.5 h under inert atmosphere

The diameters of these pores were less than 1 μm and formed along the fiber longitudinal axis. The outside surface of PCS fiber was smooth and there was no remarkable crack. Those of HSah15 fibers, however, included slight wrinkles and tiny cracks. Although HSah15 held the amount of pores, the average tensile strength after 1273 K pyrolysis was higher than 1.5 GPa.

Figure 7 shows the FE-SEM images of PCS and HSah15 fibers re-pyrolyzed at 1773 K in 30 min after 1273 K pyrolysis under inert atmosphere. The PCS fiber was white green color. On the surface of PCS, coarse *β*-SiC crystals existed and the crystals grew up on the outside of the fiber. Inner area of the fiber, however, did not show indication of SiC crystallite growth. In the case of HSah15 fiber, the color of the fiber was dark gray. There was no remarkable *β*-SiC crystals on the outside surface of the fiber. Crystal growth proceeded not only at the fiber surface, but also at an inner core area in the fiber. The whole fiber became

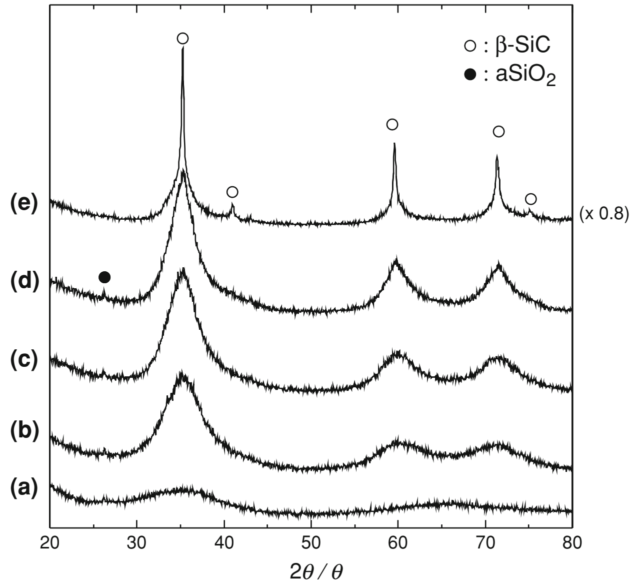

Fig. 8 The X-ray diffraction patterns (CuKα) of PCS fibers after pyrolysis under inert atmosphere (*a*) 1273 K, (*b*) 1473 K, (*c*) 1573 K, (*d*) 1673 K, (*e*) 1773 K

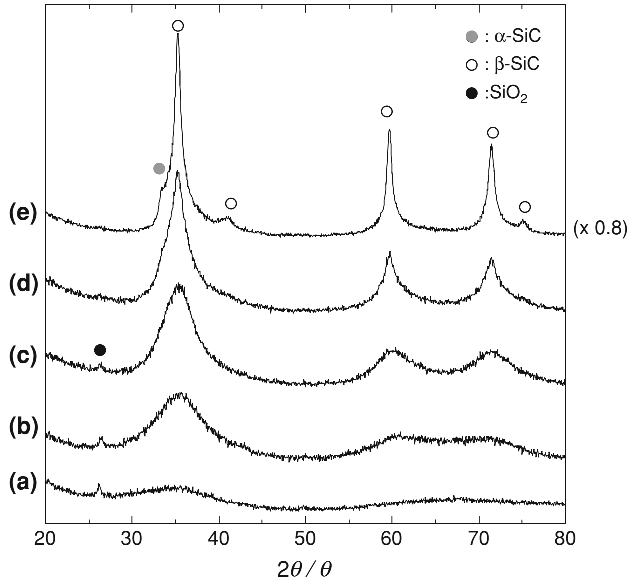

Fig. 9 The X-ray diffraction patterns (CuKα) of HSah15 fibers after pyrolysis under inert atmosphere (*a*) 1273 K, (*b*) 1473 K, (*c*) 1573 K, (*d*) 1673 K, (*e*) 1773 K

crystalline with 50–100 nm crystallite sizes. It is suspected that the component of Si–O–Si bonds in siloxane homogeneously dispersed in the fiber promote the homogeneous crystallization in the fibers derived from the polymer blends.

Figures 8 and 9 show the X-ray diffraction patterns (CuKα) of the HSah15 fibers by thermal oxidation curing after pyrolysis at 1273 K and re-pyrolyzed at 1473–1773 K under inert atmosphere (Fig. 8: PCS, Fig. 9: HSah15). The diffraction lines at $2\theta = 35°$, 60°, and 72° reveal β-SiC structure, which are sharpened as heat-treatment temperature increases [12, 13]. These fibers usually contained a small amount of silica (crystobalite) in their structure. It is obvious by a line at 22°. The fibers with nano-sized pores apparently contained large amount of silica-like structure, which was expectable from siloxane introduction in the starting precursor fibers. In addition, indication of stacking faults (α-SiC like region: 34.2°) was observed in nano-sized pore fiber after re-pyrolysis at 1773 K [14]. The results are consistent with the results of mass residue after re-pyrolysis and homogeneous crystal growth observed in SEM images.

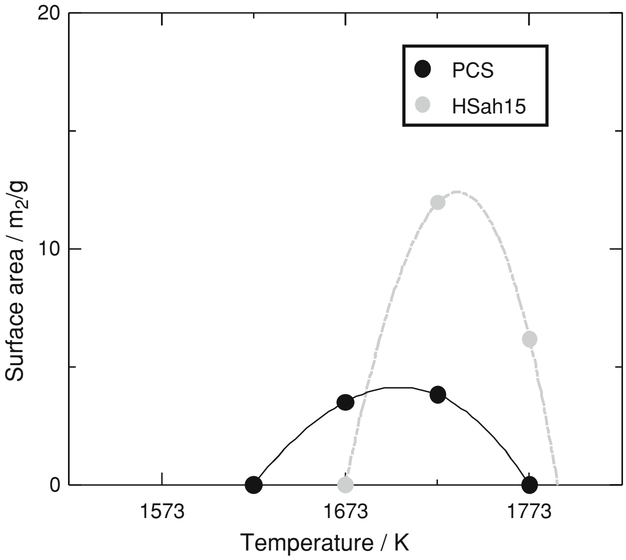

Fig. 10 The surface areas of HSah15 fibers after pyrolysis after 1573–1773 K

Figure 10 shows the specific surface areas of PCS and HSah15 fibers after re-pyrolysis after 1623–1773 K. The surface area of PCS after re-pyrolysis moderately increased at 1673 and 1723 K, while that of HSah15 increased suddenly at 1723 K and turned to decrease at 1773 K. Increased surface area at 1723 K was consistent with the observed nanoporous structure after re-pyrolysis. At 1673 K, however, fiber surface decomposition process might be suppressed in the case of HSah15.

Figure 11 shows the FE-SEM images of the cross section of the HSah15 fibers re-pyrolyzed at 1723 and re-pyrolyzed at 1773 K. The size of the crystals in the HSah15 fiber re-pyrolyzed at 1723 K was smaller than that in the HSah15 fiber re-pyrolyzed at 1773 K, and this result is reasonable when considering Fig. 10. Crystal growth in the HSah fiber at 1773 K diminished the surface area. The absolute value, however, exceeds that of the PCS fiber even after crystal growth.

It appears that silica-like domains from siloxane chains in fibers acts as nucleation sites for fiber crystallization. During high-temperature heat treatment, homogeneous crystal growth in Si–C–O amorphous proceeded to form homogeneous porous microstructure at the final stage. On the other hand, nucleation site for crystal growth in the fiber derived from PCS is limited at fiber surface area. Thus coarse grains were formed at the fiber surface, which diminish fiber strength suddenly as serious defects. It is probably a reason of maintained strength in the fibers with pores after high-temperature heat treatment.

Conclusion

The fibers with porous structure were synthesized from PCS–PMHS-h polymer blends by adjusting melt viscosity and an amount of gas evolution (mainly hydrogen) from the polymer melt. The tensile strength of the obtained

Fig. 11 The cross section of HSah15 fibers after pyrolysis after 1723 and 1773 K

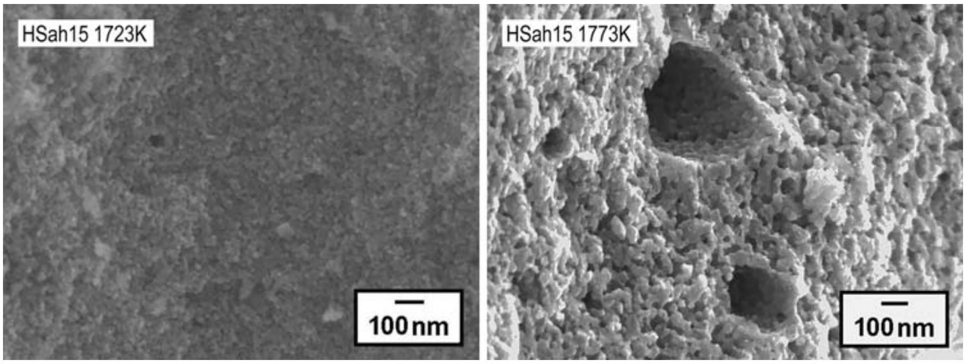

fibers with porous structure was 80% of Si–C–O fiber derived from PCS in the same synthesis conditions. This is reasonable range for fiber utilization at high-temperature region. In addition, the obtained fiber maintained strength even after 1773 K re-pyrolysis, while the fiber derived from PCS is ruptured suddenly. It is explained by homogeneous crystal growth in the fibers with pores, although the absolute mass loss is remarkable as compared with the ordinary fibers.

Acknowledgement This work is partly supported by a Grant-in Aid for Scientific Research C from Japan Society of Promotion Science.

References

1. Kita K, Narisawa M, Mabuchu H, Itoh M, Sugimoto M, Yoshikawa M (2009) J Am Ceram Soc 92:1192
2. Masuda M, Mabuchi H, Tsuda H, Matsui T, Morii K (2002) Mater Sci Forum 389–393:763
3. Kita K, Narisawa M, Mabuchu H, Itoh M, Sugimoto M, Yoshikawa M (2009) Adv Mater Res 66:5
4. Shibata K, Oi T, Otsuka A, Sumimoto H, Oshihara K, Teraoka Y, Ueda W (2003) J Ceram Soc Jpn 111:852
5. Taki T, Okamura K, Sato T (1989) J Mater Sci 24:1263. doi: 10.1007/BF02397056
6. Bouillon E, Langlais F, Pailler R, Naslain R, Cruege F, Huong PV, Sarthou JC, Delpuech A, Laffon C, Lagarge P, Monthioux M, Oberlin A (1991) J Mater Sci 26:1333. doi:10.1007/BF00544474
7. Hasegawa Y, Iimura M, Yajima S (1980) J Mater Sci 15:720. doi: 10.1007/BF00551739
8. Carberry E, West R (1966) J Organomet Chem 6:582
9. Bouillon E, Mocare D, Villenuve F, Pailler R, Naslain R, Monthioux M, Oberlin A, Guimon C, Pfister G (1991) J Mater Sci 26:1517. doi:10.1007/BF00544661
10. Simon G, Bunsell RA (1984) J Mater Sci 19:3649. doi:10.1007/BF02396937
11. Bodet R, Jia N, Tressler RE (1995) J Eur Ceram Soc 15:997
12. Hasegawa Y, Okamura K (1983) J Mater Sci 18:3633. doi: 10.1007/BF00540736
13. Shimoo T, Toyoda F, Okamura K (2000) J Am Ceram Soc 83:1450
14. Hao YJ, Jin GQ, Han XD, Guo XY (2006) Mater Lett 60:1334